Supporting Information

Honeycomb-Structured Mixed-Valence LiV_3O_8/C with Cathode-Anode Bifunctionality for Lithium-Ion Batteries

Yi Tan[a]#, Yuting Wang[a]#, Pengju Li[a]*, Jingsong Zhou[b], Jiayue Shi[a], Xiaobin Xian[a], Cunyuan Pei[a], Bing Sun[a], Dongmei Zhang[a], Shibing Ni[a]*

[a] College of Materials and Chemical Engineering, Three Gorges University, Yichang, 443002, PR China

[b] Baiyang Industrial Park Management Office, Yichang, 443000, PR China

#These authors contributed equally to this work.

*Corresponding author.

E-mail addresses: lipengju11@126.com (P. Li); shibingni07@126.com (S. Ni).

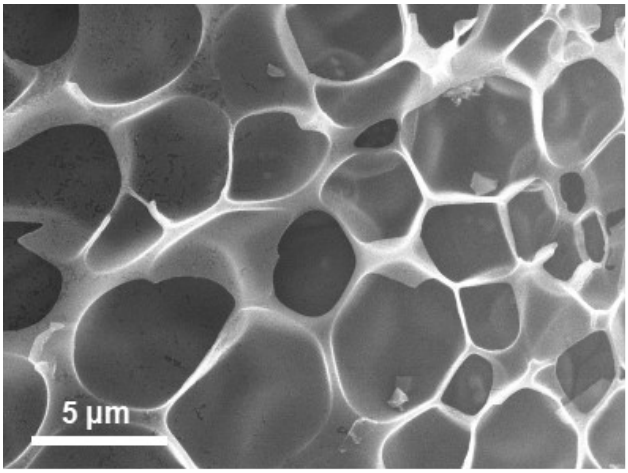

Fig. S1 The SEM image of the Li_3VO_4/C.

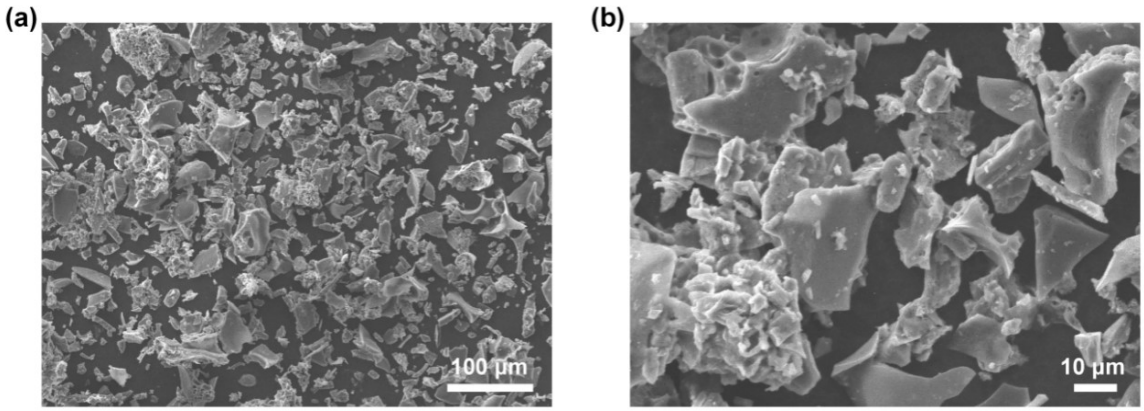

Fig. S2 SEM images of LiV_3O_8/C.

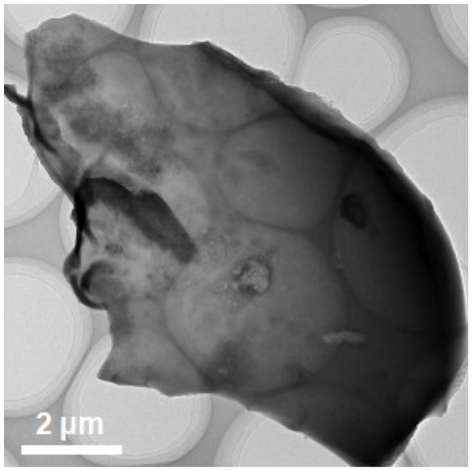

Fig. S3 TEM image of LiV_3O_8/C.

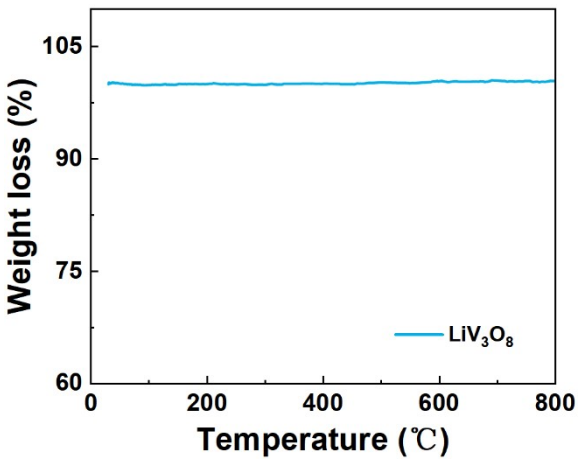

Fig. S4 TG curve of pure LiV_3O_8.

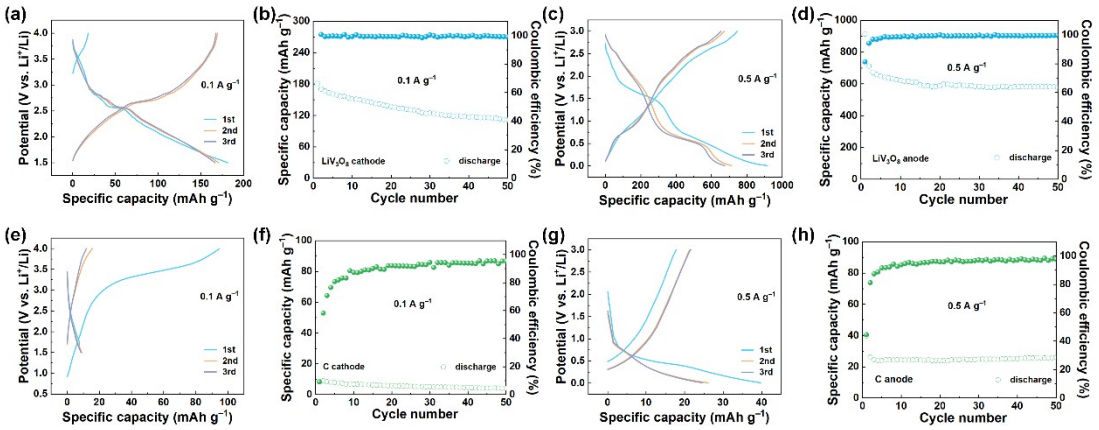

Fig. S5 Electrochemical performance of LiV_3O_8 and coating carbon electrodes. Charge-discharge profiles of (a) LiV_3O_8 cathode at 0.1 A g^{-1} and (c) LiV_3O_8 anode at 0.5 A g^{-1}. Cycling performance of (b) LiV_3O_8 cathode at 0.1 A g^{-1} and (d) LiV_3O_8 anode at 0.5 A g^{-1}. Charge-discharge profiles of (e) coating carbon cathode at 0.1 A g^{-1} and (g) coating carbon anode at 0.5 A g^{-1}. Cycling performance of (f) coating carbon cathode at 0.1 A g^{-1} and (h) coating carbon anode at 0.5 A g^{-1}.

To clarify the respective capacity contributions of LiV_3O_8 and coating carbon, the electrochemical performances of LiV_3O_8 and coating carbon were evaluated. As shown in Fig. S5, LiV_3O_8 exhibits reversible lithium insertion and extraction in both cathodic and anodic regions, but shows inferior cycling stability compared with H-LiV_3O_8/C composite, indicating the enhanced electrochemical reversibility and structural stability by the coating carbon. Meanwhile, the coating carbon delivers a negligible capacity as the cathode and approximately 26 mAh g^{-1} as the anode, whereas LiV_3O_8 delivers about 180 mAh g^{-1} as the cathode and about 600 mAh g^{-1} as the anode. Thermogravimetric analysis determines a carbon content of approximately 10.2 wt% in the composite (Fig. 2c), corresponding to a mass-weighted capacity contribution of only ~2.6 mAh g^{-1} from the coating carbon. Accordingly, it can be reasonably concluded that LiV_3O_8 is the predominant contributor to capacity in both cathodic and anodic operation, while the coating carbon primarily acts as conductive and structural-stabilizing component with negligible intrinsic lithium-storage contribution.

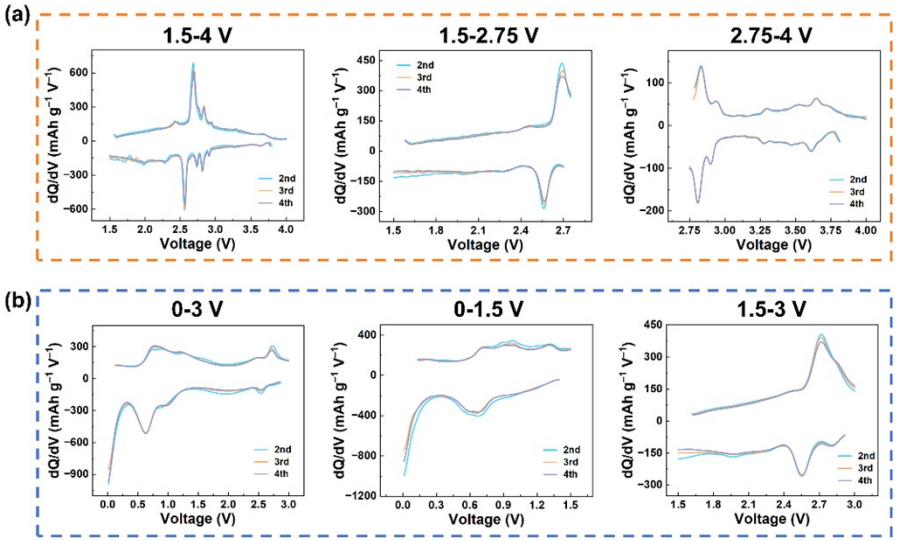

Fig. S6 The dQ/dV profiles of H-LiV_3O_8/C recorded in (a) the cathodic region (1.5~4.0 V) and (b) the anodic region (0~3.0 V). Multiple well-resolved redox peaks are observed in both voltage regions, evidencing stepwise Li^+ intercalation/extraction processes within the LiV_3O_8 framework.

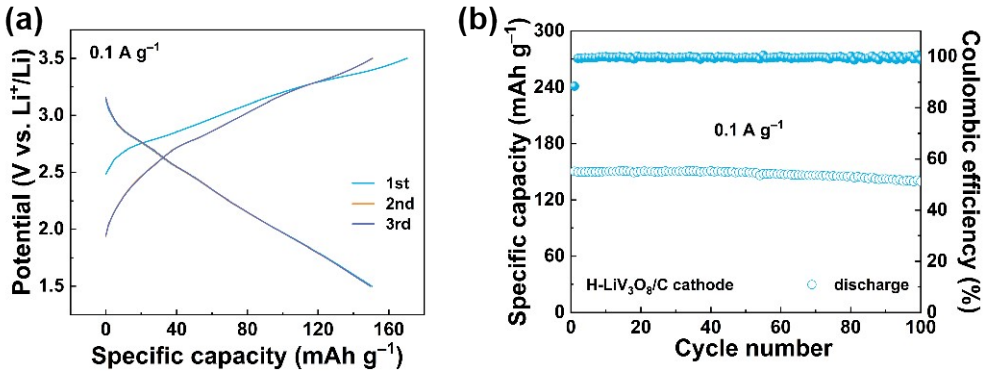

Fig. S7 (a) Charge-discharge profiles and (b) cycling performance of H-LiV_3O_8/C cathode within a voltage window of 1.5~3.5 V at 0.1 A g^{-1}.

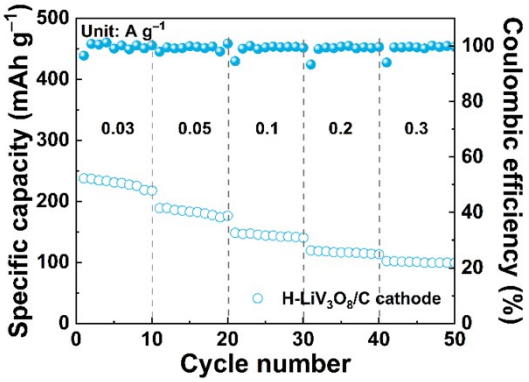

Fig. S8 Rate capability of H-LiV_3O_8/C cathode.

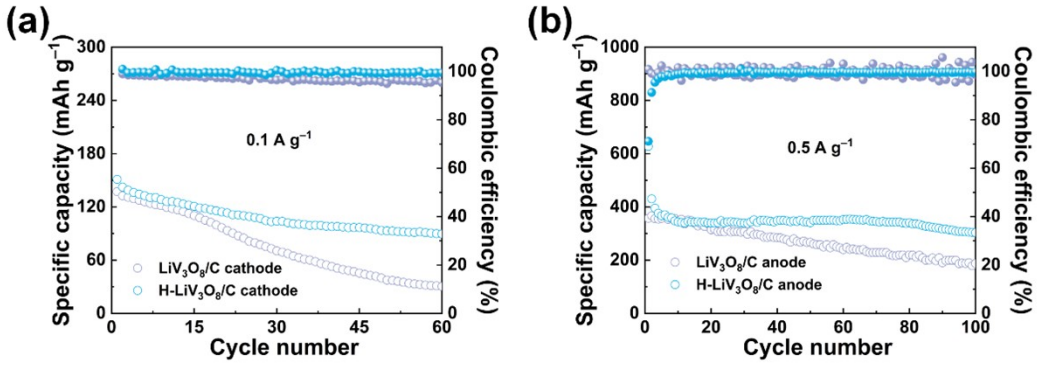

Fig. S9 Cycling performance of (a) H-LiV_3O_8/C and LiV_3O_8/C cathodes at 0.1 A g^{-1} and (b) H-LiV_3O_8/C and LiV_3O_8/C anodes at 0.5 A g^{-1} evaluated under limited lithium (50 μm Li foil) and lean electrolyte (30 μL) conditions as well as at high mass loadings (~8 mg cm^{-2}).

To further assess the reliability of bipolar electrochemical performance, the cycling performance of H-LiV_3O_8/C as both cathode and anode was evaluated under limited lithium and electrolyte as well as at high mass loading (~8 mg cm^{-2}). As shown in Fig. S9a, H-LiV_3O_8/C cathode delivers a reversible capacity of 89.6 mAh g^{-1} after 60 cycles at 100 mA g^{-1}, corresponding to a capacity retention of 59.3%. Similarly, H-LiV_3O_8/C anode maintains a reversible capacity of 303.3 mAh g^{-1} after 100 cycles at 500 mA g^{-1} (Fig. S9b). In contrast, LiV_3O_8/C suffers from rapid capacity decay under the same limited conditions. These results confirm that the dual-functional capability of H-LiV_3O_8/C is well preserved even with limited lithium and electrolyte supply, underscoring the structural reliability of the honeycomb-like architecture.

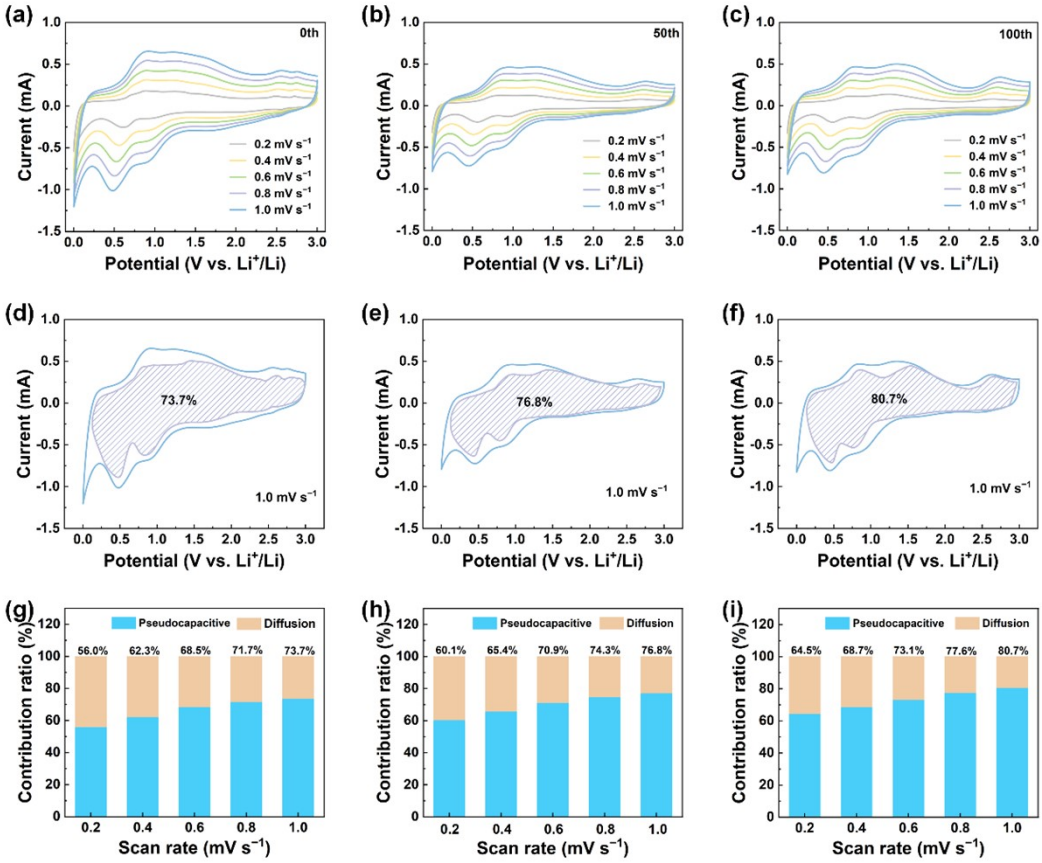

Fig. S10 Kinetics analysis of the electrochemical behavior of the H-LiV_3O_8/C electrode at different states. (a-c) CV curves of H-LiV_3O_8/C anodes at different scan rates. (d-f) Corresponding capacitive contribution to charge storage at 1.0 mV s^{-1}. (g-i) Capacitive contribution as a function of scan rate for H-LiV_3O_8/C anodes.

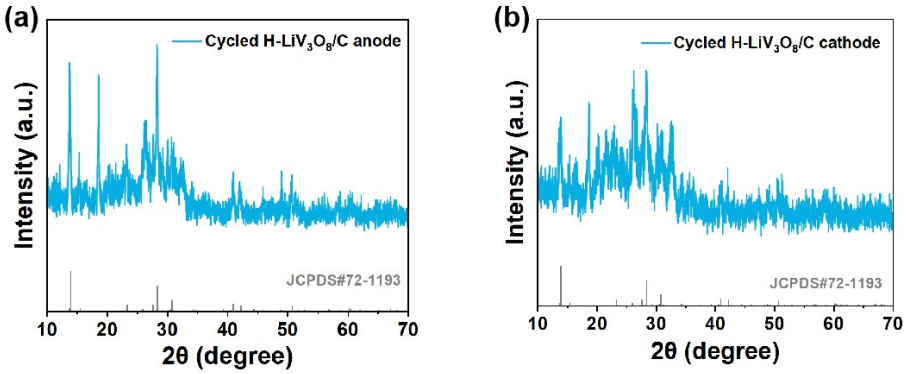

Fig. S11 XRD patterns of cycled H-LiV_3O_8/C (a) anode and (b) cathode obtained from half cells after 100 cycles.

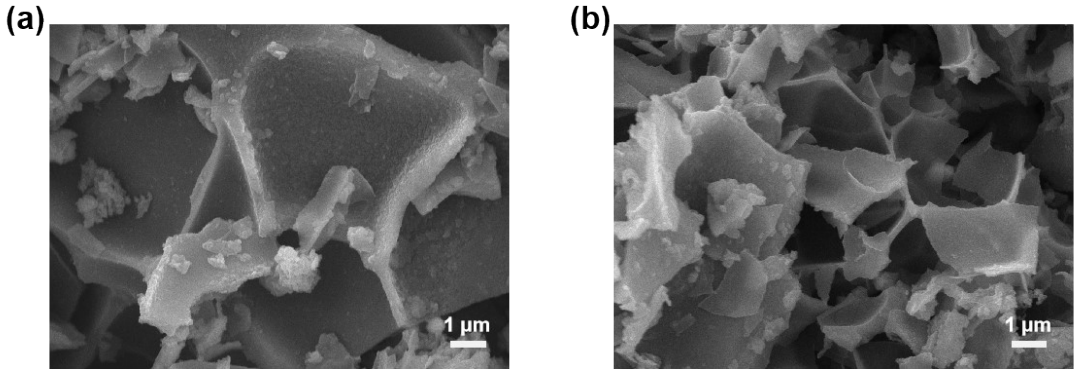

Fig. S12 SEM images of cycled H-LiV_3O_8/C (a) anode and (b) cathode obtained from half cells after 100 cycles.

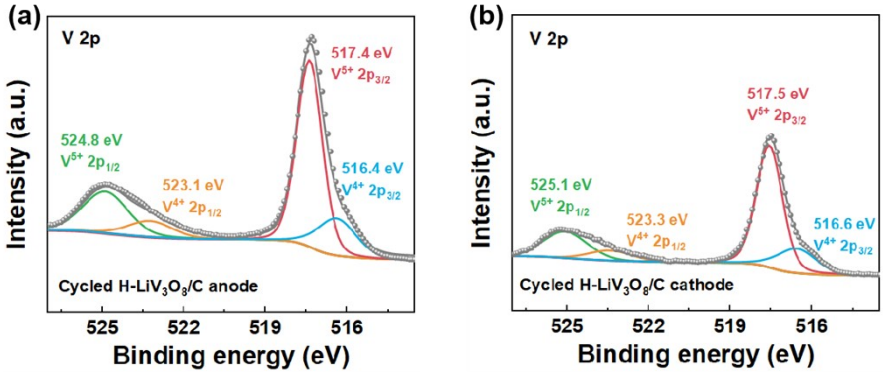

Fig. S13 V 2p XPS spectra of cycled H-LiV_3O_8/C (a) anode and (b) cathode obtained from half cells after 100 cycles.

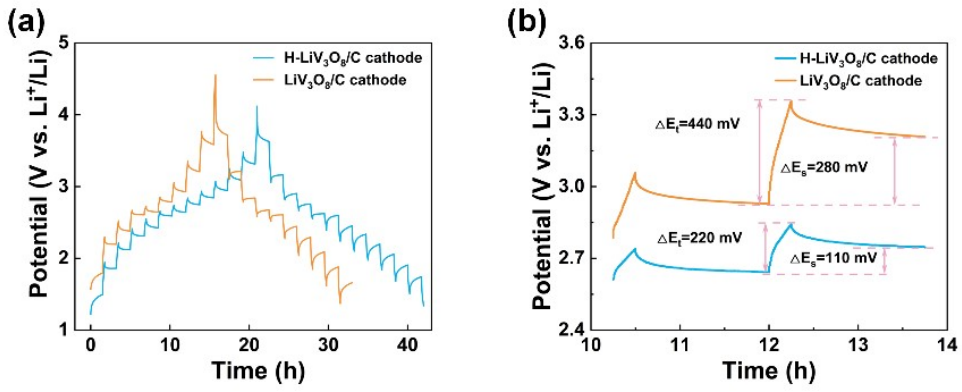

Fig. S14 (a) GITT profiles of the H-LiV_3O_8/C and LiV_3O_8/C cathode, (b) a single GITT procedure for the electrodes during the discharge process

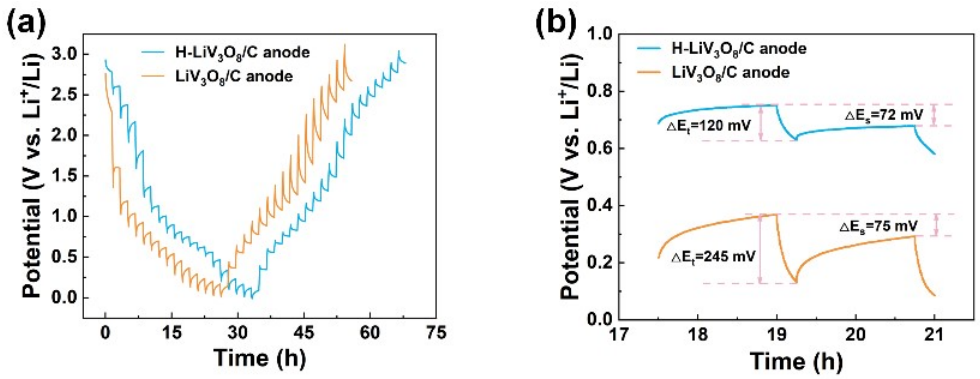

Fig. S15 (a) GITT profiles of the H-LiV_3O_8/C and LiV_3O_8/C anode, (b) a single GITT procedure for the electrodes during the discharge process

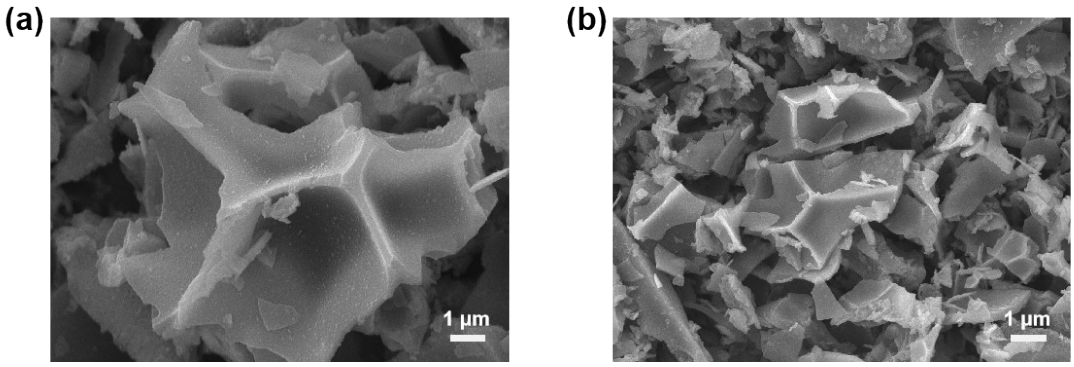

Fig. S16 SEM images of cycled H-LiV_3O_8/C (a) anode and (b) cathode obtained from full cells after 100 cycles.

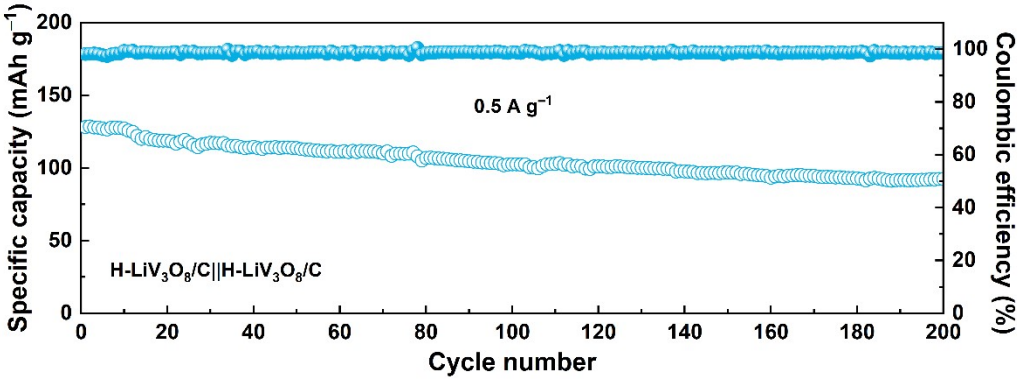

Fig. S17 Cycling performance of high-areal-loading H-LiV_3O_8/C||H-LiV_3O_8/C full cell with anode and cathode loadings of ~2.5 mg cm^{-2} and ~8 mg cm^{-2}, respectively. The specific capacity is calculated based on the mass of H-LiV_3O_8/C anode.

Table S1. Comparison of electrochemical performance of LiV_3O_8-based electrode materials reported in recent literature and this work.

Electrode type	Electrode materials	Current density (mA g^{-1})	Specific Capacity (mAh g^{-1})	Cycle number	Reference
Anode	C-LiV_3O_8/LiV_2O_5	125	546	25	*Appl. Nano Mater.*, **2023**, 6, 20258-20268.[1]
	LiV_3O_8	200	542	600	*J. Power Sources*, **2019**, 424, 158-164.[2]
	LiV_3O_8@C	300	~20	60	*Int. J. Electrochem. Sci.*, **2024**, 19, 100775.[3]
	Polypyrrole coated LiV_3O_8	500	87.2	100	*Nano Energy*, **2018**, 44, 164-173.[4]
	LiV_3O_x within carbon nanofibers - 500 ℃	500	542.7	200	*J. Colloid Interface Sci.*, **2020**, 580, 21-29.[5]
	Honeycomb-like carbon-coated LiV_3O_8	**500**	**568.2**	**200**	**This work**
Cathode	LiV_3O_8-500℃	20	118	20	*J. Mater. Eng. Perform.*, **2020**, 29, 2542-2550.[6]
	LiV_3O_8-LiV_6O_{15}	20	114.8	100	*Rare Met.*, **2025**, 44, 2815-2821.[7]
	LiV_3O_8-300℃	30	118.4	300	*ACS Appl. Nano Mater.*, **2022**, 6, 622-632.[8]
	$Li_{1+x}V_3O_8$	60	252	50	*J. Mater. Chem. A*, **2021**, 9, 1845-1858.[9]
	Ca-doped LiV_3O_8	150	170.2	400	*Nanoscale*, **2020**, 12, 10205-10215.[10]
	Microstructured LiV_3O_8	100	143.5	100	*ACS Appl. Nano Mater.*, **2023**, 6, 20258-20268.[11]
	Honeycomb-like carbon-coated LiV_3O_8	**100**	**114.8**	**100**	**This work**

References

1. A. B. Kanagaraj, A. Chandrakant Lokhande, D. A. Hussain and D. S. Choi, *Mater. Res. Bull.*, **2025**, 187, 113376.https://doi.org/10.1016/j.materresbull.2025.113376
2. L. Du, H. Lin, Z. Ma, Q. Wang, D. Li, Y. Shen, W. Zhang, K. Rui, J. Zhu and W. Huang, *J. Power Sources*, **2019**, 424, 158-164.https://doi.org/10.1016/j.jpowsour.2019.03.103
3. Z. Chen, X. Wang, Z. Zhang, S. Li, L. Zhi, G. Wang and Y. Wang, *Int. J. Electrochem. Sci.*, **2024**, 19, 100775.https://doi.org/10.1016/j.ijoes.2024.100775
4. Z. Liu, H. Li, M. Zhu, Y. Huang, Z. Tang, Z. Pei, Z. Wang, Z. Shi, J. Liu, Y. Huang and C. Zhi, *Nano Energy*, **2018**, 44, 164-173.https://doi.org/10.1016/j.nanoen.2017.12.006
5. T. Liu, T. Yao, L. Li, L. Zhu, J. Wang, F. Li and H. Wang, *J. Colloid Interface Sci.*, **2020**, 580, 21-29.https://doi.org/10.1016/j.jcis.2020.06.111
6. M. I. Ishak, M. S. Idris, R. A. M. Osman, S. M. Hasanaly, A. H. Hashim, M. F. Rosle and K. R. Ahmad, *J. Mater. Eng. Perform.*, **2020**, 29, 2542-2550.https://doi.org/10.1007/s11665-020-04727-8

7. Y. H. Zhao, Z. Q. Dai, C. W. Yang, D. Xu, J. Zhao, S. H. Chen, J. Yi, Y. P. Lei, X. Y. Zhang and J. Q. Qin, *Rare Met.*, **2025**, 44, 2815-2821.https://doi.org/10.1007/s12598-024-03121-w
8. Y. Niu, L. Xie, T. Zhou, J. Xu, Y. Ding, Q. Han, X. Qiu, Y. Xiao, Y. Miao, L. Zhu and X. Cao, *ACS Appl. Nano Mater.*, **2022**, 6, 622-632.https://doi.org/10.1021/acsanm.2c04736
9. P. Ge, S. Yuan, W. Zhao, L. Zhang, Y. Yang, L. Xie, L. Zhu and X. Cao, *J. Mater. Chem. A*, **2021**, 9, 1845-1858.https://doi.org/10.1039/d0ta10755g
10. Y. Xu, X. Wang, Z. Wang, S. Wang, X. Zhu, D. Li and J. Yu, *Nanoscale*, **2020**, 12, 10205-10215.https://doi.org/10.1039/d0nr01675f
11. R. Jiang, Z. Ding, J. Huang, Y. Xie, J. Wen, Y. Ren, Z. Liu, B. Xiao and X. Zhou, *ACS Appl. Nano Mater.*, **2023**, 6, 20258-20268.https://doi.org/10.1021/acsanm.3c04131